

A highly discriminatory RNA strand-specific assay to facilitate analysis of the role of *cis*-acting elements in foot-and-mouth disease virus replication

Samuel J. Dobson, Joseph C. Ward, Morgan R. Herod, David J. Rowlands and Nicola J. Stonehouse*

Abstract

Foot-and-mouth-disease virus (FMDV), the aetiological agent responsible for foot-and-mouth disease (FMD), is a member of the genus *Aphthovirus* within the family *Picornaviridae*. In common with all picornaviruses, replication of the single-stranded positive-sense RNA genome involves synthesis of a negative-sense complementary strand that serves as a template for the synthesis of multiple positive-sense progeny strands. We have previously employed FMDV replicons to examine viral RNA and protein elements essential to replication, but the factors affecting differential strand production remain unknown. Replicon-based systems require transfection of high levels of RNA, which can overload sensitive techniques such as quantitative PCR, preventing discrimination of specific strands. Here, we describe a method in which replicating RNA is labelled *in vivo* with 5-ethynyl uridine. The modified base is then linked to a biotin tag using click chemistry, facilitating purification of newly synthesised viral genomes or anti-genomes from input RNA. This selected RNA can then be amplified by strand-specific quantitative PCR, thus enabling investigation of the consequences of defined mutations on the relative synthesis of negative-sense intermediate and positive-strand progeny RNAs. We apply this new approach to investigate the consequence of mutation of viral *cis*-acting replication elements and provide direct evidence for their roles in negative-strand synthesis.

INTRODUCTION

The *Aphthovirus* foot-and-mouth disease virus (FMDV) is a member of the *Picornaviridae* family of single-stranded positive sense RNA viruses. FMDV is the aetiological agent of foot-and-mouth disease (FMD) and comprises seven serotypes; A, O, Asia 1, Southern African Territories (SAT) 1, SAT 2, SAT 3 and C (although believed to be extinct in the wild), which are together responsible for endemic infection in large parts of Africa, Asia and the Middle East [1]. Whilst FMD is rarely fatal, its consequences of reduced animal productivity, restriction of trade, and slaughter of infected and at-risk animals result in severe economic losses [2, 3]. The threat to maintenance of virus-free status in non-endemic regions is exacerbated by the high transmissibility of FMDV. Control measures following introduction of FMD into non-endemic regions, including strict movement restriction and mass culling, can result in costs of £billions [3–5]. The antigenic diversity of FMDV adds to the challenges of disease control, with little cross-protection provided by strain-specific vaccines and no effective therapeutics currently available [2, 6–10]. There is therefore a need to better understand the viral lifecycle in order to develop novel methods of control.

The genome of FMDV is approximately 8.4 kb and encodes a single polyprotein that is processed by viral proteases to generate the proteins required for genome replication and encapsidation. Primary cleavage of the polyprotein occurs at three positions to generate four products, the leader protease (L^{pro}), the viral structural protein precursor P1-2A and the non-structural protein precursors P2 (2BC) and P3 (3AB_{1,2,3}CD). Cleavage of L^{pro} occurs auto-catalytically, while release of the P1-2A precursor from the polyprotein occurs through a co-translational 2A-dependent ribosome skipping mechanism. The P1-2A region encodes the viral structural proteins VP1, VP3 and VP0 (the last is cleaved into VP2 and VP4 during virion maturation). Subsequent processing

Received 26 January 2023; Accepted 15 June 2023; Published 12 July 2023

Author affiliations: *School of Molecular and Cellular Biology and Astbury Centre for Structural Molecular Biology, Faculty of Biological Sciences, University of Leeds, Leeds LS2 9JT, UK.

***Correspondence:** Nicola J. Stonehouse, n.j.stonehouse@leeds.ac.uk

Keywords: cre; FMDV; foot-and-mouth disease virus; negative sense; replication; strand-specific assay.

Abbreviations: 5-EU, 5-ethynyl uridine; FMD, foot-and-mouth disease; FMDV, foot-and-mouth disease virus; ptGFP, ptilosarcusGFP; qPCR, quantitative PCR; ssRT, strand-specific reverse transcription; UTR, untranslated region.

Five supplementary tables are available with the online version of this article.

001871 © 2023 The Authors



This is an open-access article distributed under the terms of the Creative Commons Attribution License. This article was made open access via a Publish and Read agreement between the Microbiology Society and the corresponding author's institution.

of the P2 and P3 precursors generates the viral non-structural proteins 2B, 2C and 3A, 3B_{1,2+3} (VPg), 3C protease (3C^{pro}) and RNA-dependent RNA polymerase (3D^{pol}) [11–21]. This processing is thought to be mediated by 3C^{pro} through alternative *cis*- and *trans*-pathways that appear to coordinate replication [17, 22, 23].

The single viral ORF is flanked by untranslated regions (UTRs) at the 5' and 3' ends of the genome. The FMDV 5' UTR is the longest amongst known picornaviruses and contains several highly structured domains that are essential to the virus lifecycle [24–30]. The S-fragment is an ~360 nt hairpin-loop that occupies the same location (at the extreme 5' end of the 5' UTR) as the cloverleaf found in enteroviruses [31–34]. It appears to be involved in immune modulation and viral replication via interactions with host and viral proteins [27, 35, 36]. Adjacent to the S-fragment is a poly-C sequence of unknown function, followed by two to four RNA pseudoknots, which appear to be involved in assembly of infectious virions in addition to genome replication [24, 37–39]. Adjacent to the pseudoknots is a small hairpin-loop known as the *cis*-acting replication element (*cre*) that in other picornaviruses is located within the ORF [25, 40]. Whilst the location of the *cre* appears not to be important, it has an indispensable role in replication [25], acting as a template for the uridylylation of VPg by 3D^{pol} [41–43]. VPg_pU_p primes genome replication by 3D^{pol} [22, 44, 45]. Finally, the internal ribosome entry site (IRES) is located immediately upstream of the ORF and is essential for initiation of translation [26, 29, 30, 46].

Picornavirus genome replication is initiated by the synthesis of a negative-sense copy of the infecting genome followed by assembly of a 'replicative intermediate' [47–49]. This complex comprises the negative-strand template RNA and several nascent progeny positive-strand RNAs together with 3D^{pol} and other viral and cellular proteins [50, 51]. There is evidence that in the native state of the replicative intermediate the nascent daughter strands are not collapsed onto the negative template strand but are only transiently associated at the site of transcription [50]. The synthesis of both negative and positive RNA strands appears to be primed with VPg_pU_p [41].

While it is well documented that the *cre* element is essential for viral replication, it is not firmly established whether this is required to produce VPg_pU_p for the priming of both negative- and positive-sense RNA molecules during intracellular virus replication. Indeed, it has been reported that priming of negative-strand RNA synthesis can occur in a *cre*-independent manner during cell-free replication of poliovirus, possibly via the poly(A) tail [52–54]. As mutation of the *cre* is lethal to progeny virus production, methods that facilitate the initiation of replicative events but are not reliant on infection (such as transfection of *in vitro* transcribed viral RNA) are useful for study of the initial steps in replication. Whilst assays to distinguish positive- and negative-strand RNAs have been developed for several viruses including FMDV, o'nyong-nyong virus, dengue virus, murine norovirus and chikungunya virus, their applications have so far been limited to studies involving infectious virus production [55–59].

Replicons are mini-genomes in which the genomic region encoding structural proteins is replaced with a reporter gene to facilitate the study of RNA replication independent of other aspects of the virus lifecycle [60]. In addition to their application in the dissection of the molecular details of replication, replicons permit the study of viruses that require high-containment facilities, such as FMDV, at lower laboratory containment. However, because the delivery of RNA by transfection is an inefficient process, large quantities of *in vitro* transcribed RNA are used to ensure that sufficient cells are transfected. This can overload subsequent strand-specific assays. Here, we describe a strand-specific quantitative (q)PCR assay using FMDV replicons to determine the effects of mutations on the synthesis of both negative and positive strands in parallel assays. We have applied this method to determine the role of the *cre* element in the initiation of synthesis of both positive- and negative-strand RNAs.

METHODS

Cell lines and maintenance

Baby hamster kidney (BHK-21) cells were purchased from ATCC (LGC Standard) and were maintained in Dulbecco's modified Eagle's medium (DMEM) with glutamine, supplemented with 10% (v/v) FBS, 50 U ml⁻¹ penicillin and 50 µg ml⁻¹ streptomycin. Growth medium and supplements were purchased from Sigma-Aldrich, Merck.

In vitro transcription

The construction, linearisation and purification of FMDV replicon plasmids has been described previously [24, 60]. Linear plasmids were transcribed *in vitro* using the T7 RiboMAX Express Large Scale RNA Production System (Promega) using 'half sized' reactions whereby 250 ng linear plasmid was added to a reaction mixture using half the volume suggested for all reagents in the manufacturer's protocol. Reactions were incubated at 37 °C for 1.5 h prior to addition of 1 µl DNase I and further incubation at 37 °C for 20 min. The resulting RNA was purified using the RNA Clean and Concentrator-25 kit (Zymo Research) prior to quantification by NanoDrop (Thermo Fisher) and confirmation of integrity by denaturing MOPS-formaldehyde gel electrophoresis.

Replication assays

BHK-21 cells were seeded into six-well plates at a density of 1×10⁶ cells per well and incubated for 16 h. After incubation, cells were transfected with *in vitro* transcribed replicon RNA using Lipofectamine 2000 (Thermo Fisher). RNA (0.5 µg cm⁻²) and

Table 1. Primers used in RT and qPCRs

Underlined are the non-viral tag sequences for both the RT and qPCR primers.

Target	Application	Name	Sequence (5'–3')
PS	RT	PS-tag-RT	<u>GCAGGAGCTAAGCGCTGGGGTCGCGATGATGACTTTGC</u>
	qPCR	PS-qPCR-TAG	<u>GCAGGAGCTAAGCGCTGG</u>
	qPCR	PS-qPCR-R	GATTTGGGCCAGAACCCTGA
NS	RT	NS-tag-RT	<u>TGACGTTGCGACGAGTTCGCCAAAGACGGAGCTGACACT</u>
	qPCR	NS-qPCR-TAG	<u>TGACGTTGCGACGAGTTCG</u>
	qPCR	NS-qPCR-R	GTCCACAATCAACCCCTCGT
β -Actin	qPCR	β -actin-F	GTGCTATGTTGCCCTGGACT
	qPCR	β -actin-R	GCTCGTTGCCAATGGTGATG

RT, reverse transcription; PS, positive-strand; NS, negative-strand; F and R refer to forward and reverse qPCR primer, respectively.

Lipofectamine 2000 (1 μ g RNA:3 μ l reagent) were added separately to 50 μ l opti-MEM (Thermo Fisher) and incubated for 10 min at room temperature. RNA and reagent were mixed and incubated for 20 min at room temperature before diluting with phenol-red-free DMEM (Thermo Fisher) supplemented with 10% (v/v) FBS and GlutaMAX (Thermo Fisher) diluted to 1 \times . Cells were washed once using PBS, before addition of transfection mixture. Cells were imaged over time using the 10 \times objective of an Incucyte S3 live cell imaging system to detect phase and green fluorescence as a measure of replication [61, 62]. Analysis was performed with the inbuilt Incucyte 2021A analysis suite using surface fit segmentation, threshold minimum (green calibrated units, GCU) 8.0, edge split sensitivity –30 and minimum area filter 50 μ m² to determine green fluorescent cells. Following incubation for 6 h, cells were washed once with PBS and extracted by addition of 1 ml TRI reagent (Merck) directly to the monolayer. Harvested cell extracts were stored at –20 °C until further processing.

RNA extraction and cDNA synthesis

Total RNA was TRI reagent-extracted from BHK-21 cells using Phasemaker tubes (Invitrogen, Thermo Fisher) and associated manufacturer's protocol. An additional 75% EtOH RNA pellet wash step was performed to ensure removal of trace contaminants prior to RNA solubilisation using nuclease-free H₂O. Contaminating DNA was removed using the TURBO DNA-free kit (Thermo Fisher) following the manufacturer's guidelines. Total RNA purity and concentration was determined by NanoDrop.

cDNA synthesis was performed using SuperScript IV Reverse Transcriptase (Thermo Fisher) following the manufacturer's guidelines unless stated otherwise. Separate reactions were performed using 2 μ M strand-specific reverse transcription (ssRT) primer (Table 1, PS-tag-RT or NS-tag-RT) or 50 μ M oligo(dT)₂₀. A total mass of 500 ng RNA was added to each reaction, together with dNTP mix containing 10 mM of each nucleotide (Promega). Combined reaction mixtures were incubated at 50 °C for 10 min prior to inactivation at 85 °C for 10 min.

qPCR assays

cDNA synthesised from total RNA was diluted 100-fold in nuclease-free H₂O unless otherwise stated. qPCR was performed using GoTaq qPCR Master Mix (Promega). Reaction mixes were made up in a 10 μ l total volume containing 500 nM forward and reverse primers (Table 1, PS-qPCR-tag and PS-qPCR-R or NS-qPCR-tag and NS-qPCR-R or β -actin-F and β -actin-R) and 2 μ l diluted cDNA. qPCR conditions followed the manufacturer's recommended fast cycling programme with polymerase activation (95 °C, 2 min) followed by 40 cycles (denaturation at 95 °C, 3 s and annealing/extension at 60 °C, 30 s) with melt curve analysis on a CFX Connect Real-Time PCR Detection System (Bio-Rad).

Nascent RNA labelling assays

Nascent RNA labelling assays were performed using the Click-iT Nascent RNA Capture Kit (Thermo Fisher). Replication assays were performed as described previously in six-well plates, with addition of 0.2 mM 5-ethynyl uridine (5-EU) diluted from a 200 mM stock, to transfection complex mixtures immediately prior to addition to cells. Cells were harvested 6 h post-transfection through the addition of 1 ml TRI reagent (Sigma-Aldrich, Merck) directly to the monolayer, with collected samples stored at –20 °C until further processing. RNA was extracted as indicated above. Biotinylation of RNA by click reaction was performed following the manufacturer's guidelines using 10 μ g total RNA and 0.5 mM biotin azide in a 50 μ l reaction. RNA was precipitated

in ammonium acetate overnight at -80°C , pelleted, washed and solubilised in nuclease-free H_2O , as recommended. RNA was quantified by NanoDrop and 1 μg biotinylated RNA was mixed with 12 μl Dynabeads MyOne Streptavidin T1 magnetic beads. Following 30 min of incubation at room temperature with agitation at 600 r.p.m., beads were washed for 3 min at room temperature with agitation at 600 r.p.m. five times using washer buffer 1 and five times using wash buffer 2, with magnetic capture performed between washes. Bead mixtures were transferred to a new tube after every three washes to minimise tube contaminant carry over. Following the final wash, beads were resuspended in 36 μl wash buffer 2 and 12 μl slurry divided between three separate tubes for separate reverse transcription of positive-strand genomes, negative-strand genomes and total poly(A) RNA. Bead suspensions were heated at 70°C for 5 min prior to immediate addition of 17 μl master mix containing 15 μl nuclease-free H_2O , 1 μl 10 mM dNTPs and 1 μl 2 μM ssRT primer (Table 1) or 50 μM oligo(dT)₂₀. Mixes were cooled to room temperature with agitation at 600 r.p.m. for 10 min before addition of 8 μl 5 \times SuperScript IV reaction buffer, 2 μl 100 mM DTT and 1 μl SuperScript IV enzyme to each reaction. Samples were incubated at 50°C for 1 h with agitation at 600 r.p.m. Reaction mixtures were heated at 85°C for 10 min to inactivate reverse transcription and release cDNA from beads. Tubes were pulse centrifuged to pellet liquid prior to bead immobilisation using a magnetic rack and aspiration of cDNA. cDNA was diluted 100-fold for positive-strand reactions and 10-fold for negative-strand reactions. Oligo(dT)₂₀ reactions were diluted accordingly. qPCRs were performed as described above with quantification using the $\Delta\Delta\text{C}_q$ method using β -actin as a reference gene. Data from each experiment were analysed individually and normalised to data from WT samples. Statistical analysis was performed by one-way ANOVA with comparison to WT using three experimental repeats. Samples in which no signal was detected were arbitrarily assigned a C_q value of 40 to permit quantification. Bars on graphs represent mean with SEM.

RESULTS

Transfection with replicon RNA is not compatible with strand-specific discrimination by qPCR

Reverse genetics is a powerful tool for investigating the molecular biology of many viruses. However, a common drawback with many reverse genetics systems is the inefficient delivery of *in vitro* transcribed viral genomes necessitating the use of large amounts of input viral RNA, which can overwhelm assays designed to dissect individual steps of viral lifecycles such as strand-specific genome synthesis. To overcome this restriction we have developed assays involving nascent RNA labelling, reverse transcription and strand-specific qPCR to examine the individual steps of negative- and/or positive-strand synthesis.

Our previously reported assays of replication utilised an FMDV replicon encoding the GFP reporter protein in place of the viral structural proteins [60, 63]. Transfection of *in vitro* transcribed replicon RNA into cells allows measurement of a completed replication cycle via GFP expression prior to RNA extraction, cDNA synthesis and measurement of strand-specific RNA replication by qPCR (Fig. 1a). Following transfection with *in vitro* transcribed pRep-ptGFP replicon RNA (WT or the replication-deficient 3D^{GNN} as a control for input translation) or yeast tRNA, cells were examined using an Incucyte S3 instrument to visualise phase contrast and green images and the number of ptilosarcus (pt) GFP-positive cells determined using pre-defined analysis parameters (Fig. 1b). The differences between GFP expression in the WT and GNN constructs was used as a measure of replication in concordance with our previous studies [24, 63, 64].

Strand-specific primers with a non-viral tag sequence were designed for use during reverse transcription reactions to generate unique 5' sequences providing specificity for each strand (Table 1) similar to published protocols [55–58]. To minimise the potential for cross-contamination, primers were designed towards the 5' and 3' ends of the FMDV replicon genome for the positive and negative strand, respectively (Fig. 1c). Reverse transcription using oligo(dT)₂₀ was also performed for each sample to permit normalisation between samples by amplifying β -actin as a stably expressed reference gene. A primer complementary to the strand-specific non-viral tag and an internal primer complementary to the viral genome were designed for the strand-specific qPCR. Specificity of primers for the intended strand was confirmed by a challenge assay, whereby a known copy number of *in vitro* transcribed replicon RNA was 'spiked' into total RNA extracted from BHK-21 cells in the presence and absence of the opposite strand (Table S1, available in the online version of this article). To mimic conditions during viral replication where the positive strand significantly outweighs the presence of the negative strand [65, 66], a low copy number of negative strand (10^3 copies μl^{-1}) was challenged with 10^5 copies μl^{-1} positive-strand RNA. As it is plausible that some mutations may prevent the synthesis of nascent positive strands but allow synthesis of the negative strand, a higher copy number of negative-strand (10^5 copies μl^{-1}) was used to challenge an equal number of positive strands. Results indicated that addition of 10^5 copies μl^{-1} opposite strands did not alter the observed C_q and therefore that assay specificity was retained. Initial assays were performed comparing strand production between WT and 3D^{GNN} replicons. As anticipated, only a ≈ 2 -fold difference was observed between WT and 3D^{GNN} for both strands (Fig. 1d, e, Table S2), suggesting that the ability to demonstrate nascent viral RNA production was masked by the large quantity of input RNA necessary to efficiently initiate replication.

Removal of input replicon genomes by nascent RNA labelling

We speculated that the inability of the strand-specific qPCR to clearly distinguish between RNA isolated from cells transfected with either replication-competent or replication-incompetent replicon constructs was due to the large amount of input RNA

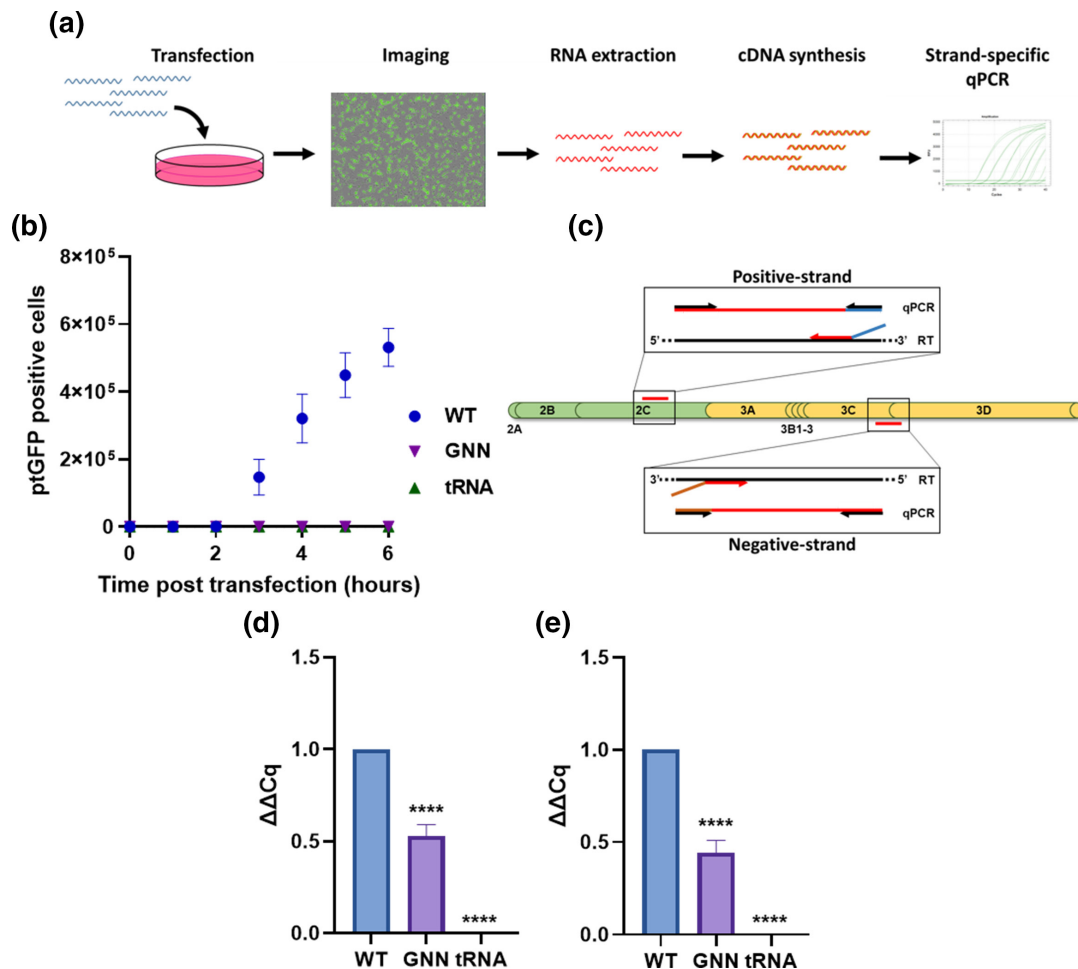


Fig. 1. Transfection of replicon is not suitable for a strand-specific assay following RNA extraction. (a) Schematic overview of a replicon transfection assay with imaging prior to RNA extraction, cDNA synthesis and strand-specific qPCR. (b) Detection over time of ptGFP following transfection of cells with WT or 3D^{GNN} FMDV pRep-ptGFP RNA or yeast tRNA control. (c) Schematic representation of primer binding regions with P2 and P3 genomic regions of FMDV for the cDNA synthesis and qPCR detection of positive and negative strands. RNA extracted from transfected cells was reverse transcribed using strand-specific primers prior to qPCR to detect positive-strand (d) and negative-strand (e) expression. Analysis was performed using the $\Delta\Delta Cq$ method relative to WT. Statistical analysis was performed by one-way ANOVA with **** $P < 0.0001$. $N = 3$.

necessary to initiate replication in the majority of the cells. To address this, we developed a method to specifically label and isolate newly synthesised RNA. To facilitate selection, transfected cells were incubated with an alkyne-modified uridine, 5-EU, from the time of transfection so that only cellular RNAs and viral genomes synthesised during replication incorporated the modified nucleotide (Fig. 2a). Control assays indicated that addition of 0.2 mM 5-EU to the culture medium did not inhibit replication (Fig. 2b). BHK-21 cells were incubated with or without 0.2 mM 5-EU prior to RNA extraction and biotinylation by click reaction. Pre- and post-click RNA was reverse transcribed and qPCR performed to determine the effect of RNA biotinylation on detection of β -actin. The results indicated that click reactions and biotin labelling had minimal effects upon qPCR detection (Table S3).

Following RNA extraction, strand-specific qPCR was performed to determine whether incorporation of 5-EU had any adverse effects upon the assay. These assays showed that detection of positive- and negative-strand genomes (Fig. 2c, d, respectively) was comparable to that observed without labelling (Fig. 1d, e). Copper-catalysed click reactions were performed to covalently link azide-modified biotin to the newly synthesised RNA. This acted as a bait for capture with streptavidin magnetic beads and removal by washing of input replicon RNA. Following capture and on-bead reverse transcription, analysis of the eluted cDNA confirmed that the method had efficiently removed replicon input RNA, with the 3D^{GNN} replicon signal reduced to 0.03 and 0.02 relative to that of WT for the positive and negative strand, respectively (Fig. 2e, f, Table S4). This confirmed that labelling of newly synthesised RNA with 5-EU prior to biotin modification by click reaction and bead capture provided a method suitable for replicon-based investigation of differential viral strand synthesis.

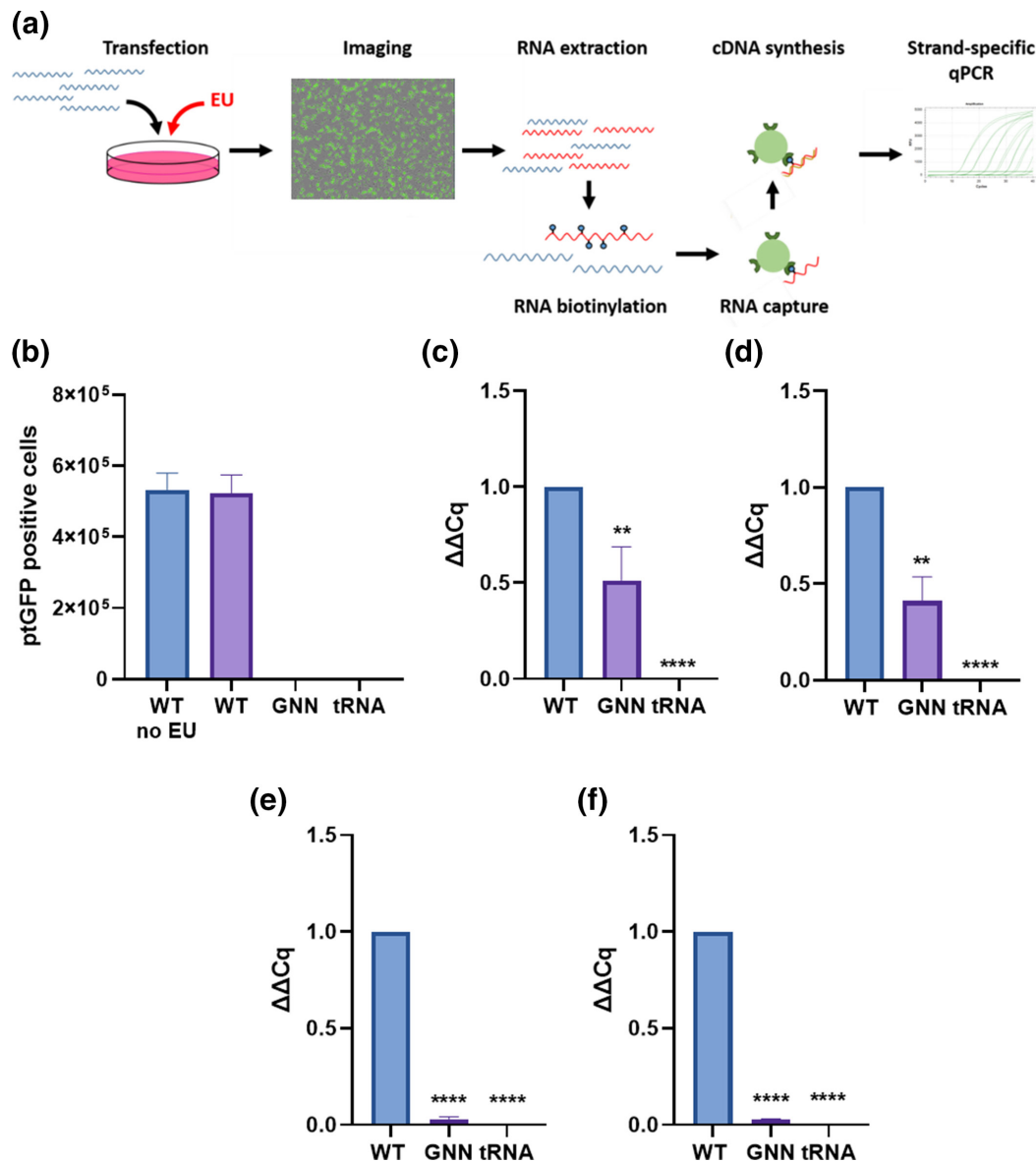


Fig. 2. Removal of input replicon RNA by 5-EU labelling and RNA pulldown to identify nascent replication. (a) Schematic representation of a 5-EU nascent RNA labelling assay. BHK-21 cells were transfected with FMDV pRep-ptGFP RNA, with addition of 0.2 mM 5-EU to label nascent RNA. Cells were imaged using an Incucyte S3 instrument prior to harvest of RNA 6 h post-transfection. Nascent RNA was biotinylated by click reaction and captured with streptavidin magnetic beads. Input RNA was removed by washing prior to on-bead cDNA synthesis and strand-specific qPCR. (b) ptGFP-positive cells detected by Incucyte S3 imaging 6 h post-transfection to determine the effect of 5-EU labelling on replication. Following RNA extraction, strand-specific qPCR was performed prior to click reaction to detect (c) positive strands and (d) negative strands. Click reaction-mediated biotinylation of nascent RNA, magnetic bead capture and on-bead cDNA synthesis was performed prior to strand-specific assays to determine positive-strand (e) and negative-strand (f) expression. Analysis was performed using the $\Delta\Delta Cq$ method relative to WT. Statistical analysis was performed by one-way ANOVA with ** $P < 0.005$ and **** $P < 0.0001$. $N = 3$.

The *cre* is essential for negative-strand production

The *cre* is essential to replication of picornaviruses by acting as a template for uridylylation of VPg by 3D^{pol}. There is also evidence that the poly(A) tail of poliovirus may act as a template for uridylylation in cell-free replication, albeit less efficiently [52–54]. However, whether *cre* is essential for VPg uridylylation to prime the synthesis of the negative-strand intermediate during FMDV replication in cells is unknown. The role of the *cre* in strand synthesis was therefore investigated using replicons harbouring a complete *cre* deletion (Δcre) or with a single nucleotide substitution of the functional AAACA motif (termed A1G, containing mutation of the first A nucleotide to G). Both of these mutations are known to prevent the complete virus lifecycle [25]. Loss of replication competency was confirmed here for both mutants by a replicon assay (Fig. 3a). Strand-specific assays confirmed

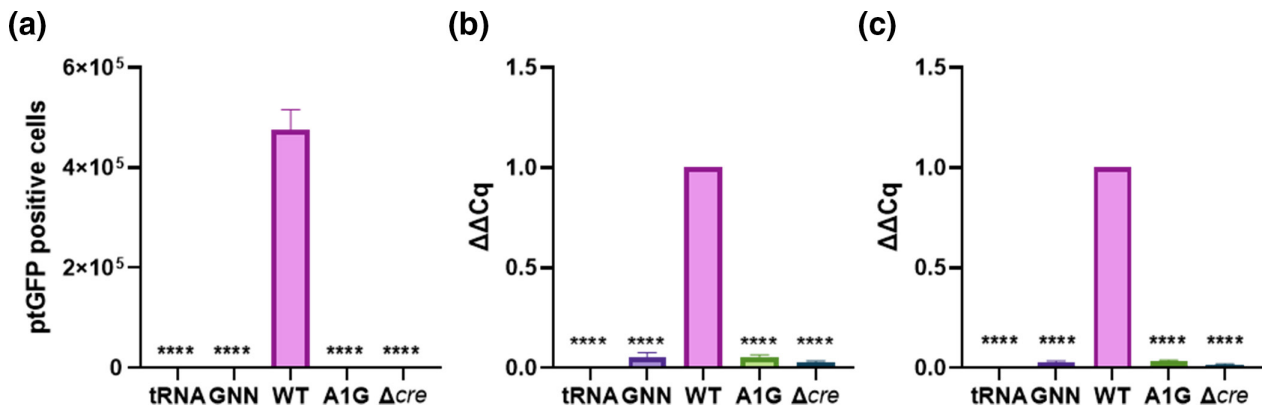


Fig. 3. FMDV *cre* is essential to the production of negative-strand genomes. (a) BHK-21 cells were transfected with pRep-ptGFP constructs containing *cre* mutations A1G and Δcre alongside controls, with addition of 0.2 mM 5-EU to label nascent transcribed RNA. ptGFP positive cells were visualised 6 h post-transfection using an Incucyte S3 instrument. Total RNA extracted 6 h post-transfection was biotinylated by click reaction, captured with streptavidin beads and reverse transcribed using strand-specific or oligo dT₍₂₀₎ as a primer. cDNA was used in strand-specific qPCR assays to determine positive-strand (b) and negative-strand (c) expression. Analysis was performed using the $\Delta\Delta Cq$ method relative to WT. Statistical analysis was performed by one-way ANOVA with **** $P < 0.0001$. $N = 3$.

that the positive strand could not be synthesised by either mutant replicon (Fig. 3b, Table S5). Negative-strand production was also ablated, showing that the *cre* is also essential during intracellular replication for production of the negative strand (Fig. 3c, Table S5).

DISCUSSION

The ability to reliably differentiate positive- and negative-strand RNAs is important for investigating details of the mechanism of picornavirus replication. This can be achieved using qPCR techniques, but the selection of strand-specific primers can be challenging. This problem is exacerbated when studying replicons, as reliable transfection requires a large quantity of input RNA. Despite these drawbacks, replicons facilitate investigations of replication that would otherwise be technically challenging, for example with non-recoverable or poorly replicating viruses, or to address issues regarding containment and safety. We therefore designed a strand-specific qPCR assay to distinguish synthesis of each strand separately within the context of such a complex environment (where the opposite strand could interfere) and explored how mutation to the viral genome may restrict synthesis.

Initial assays identified the large quantity of input RNA required to ensure transfection of the majority of cells as a major restriction to demonstrating differences between replication-competent and replication-defective replicons (Fig. 1). In the case of the FMDV replicon, the ≈ 7 kb genome relates to approximately 1.8×10^{12} genome copies μg^{-1} , and with up to 5 μg per well of replicon being transfected into cells, carry-over of input RNA was unsurprising. RNA self-priming, a consequence of high secondary structure at the 3' terminus of RNA and reverse transcriptase lacking RNase H activity, has been reported previously as a source of contamination by complementary sequences in strand-specific assays [57, 58]. In addition, residual fragments of plasmid DNA used as template for *in vitro* transcription of the transfecting RNA could theoretically also be a source of contaminating complementary sequences. However, contamination by any interfering sequences is eliminated by the specific selection of newly synthesised RNA as described here, thus providing an assay that can reliably distinguish complementary strands. It should be noted that there are differences in sensitivities in the detection of the strands. However, as the detection of these is achieved in separate reactions, it would not be appropriate to make direct comparisons.

The essential role of the *cre* in picornavirus replication is well documented and was also confirmed here in replicon assays (Fig. 3a) [36, 52–54, 67]. It is possible that the poly(A) tail could template uridylylation of VPg (i.e. in addition to and independently of the *cre*, as reported in cell-free assays) [52–54]. However, it was not established whether the *cre* is required for negative-strand synthesis in an intracellular assay. We therefore investigated the role of two *cre* mutations (A1G and Δcre) during strand synthesis and found that neither positive- nor negative-strand RNAs were transcribed. Given that negative-strand intermediates were not produced, it is unsurprising that positive-strand production was also restricted. Due to a lack of negative-strand RNA it could not be established in this assay whether synthesis of new positive-strand genomes requires the *cre*. However, given evidence from the literature of the importance to positive-strand RNA synthesis, these findings would suggest that the *cre* is essential for efficient priming of replication by 3D^{pol} in the infected cell.

In conclusion, we present a technique which employs 5-EU labelling and purification of nascent RNA prior to strand-specific qPCR that can be applied to determine the role of viral elements in transcription of positive and negative strands using replicons

containing specific mutations. Here, this was applied to the known *cre* mutations A1G and Δcre and results suggested that neither are capable of producing a negative-strand intermediate. We will continue to probe other mutants to discover the role of viral elements that control viral replication of positive and negative strands.

Funding information

This project was funded by the Biotechnology and Biological Sciences Research council UK (project grant reference BB/T015748/1).

Acknowledgements

We are grateful to group members for their helpful comments on the project. Thanks to Andrew Macdonald for access to equipment funded by MR/S001697/1.

Author contributions

The project was conceived by S.J.D., M.R.H., D.J.R and N.J.S. The experiments were carried out and the data analysed by S.J.D. J.C.W undertook mutagenesis. The manuscript was drafted by S.J.D and was edited and revised by all authors.

Conflicts of interest

The authors declare that there are no conflicts of interest.

References

1. Paton DJ, Di Nardo A, Knowles NJ, Wadsworth J, Pituco EM, *et al.* The history of foot-and-mouth disease virus serotype C: the first known extinct serotype? *Virus Evol* 2021;7:veab009.
2. Jamal SM, Belsham GJ. Foot-and-mouth disease: past, present and future. *Vet Res* 2013;44:116.
3. Knight-Jones TJD, Rushton J. The economic impacts of foot and mouth disease - what are they, how big are they and where do they occur? *Prev Vet Med* 2013;112:161–173.
4. Feng S, Patton M, Davis J. Market Impact of foot-and-mouth disease control strategies: a UK case study. *Front Vet Sci* 2017;4:129.
5. Thompson D, Muriel P, Russell D, Osborne P, Bromley A, *et al.* Economic costs of the foot and mouth disease outbreak in the United Kingdom in 2001. *Rev Sci Tech* 2002;21:675–687.
6. Mahapatra M, Parida S. Foot and mouth disease vaccine strain selection: current approaches and future perspectives. *Expert Rev Vaccines* 2018;17:577–591.
7. Park J-H. Requirements for improved vaccines against foot-and-mouth disease epidemics. *Clin Exp Vaccine Res* 2013;2:8–18.
8. Stenfeldt C, Eschbaumer M, Rekant SI, Pacheco JM, Smoliga GR, *et al.* The foot-and-mouth disease carrier state divergence in cattle. *J Virol* 2016;90:6344–6364.
9. Dawe PS, Flanagan FO, Madekurozwa RL, Sorensen KJ, Anderson EC, *et al.* Natural transmission of foot-and-mouth disease virus from African buffalo (*Syncerus caffer*) to cattle in a wildlife area of Zimbabwe. *Vet Rec* 1994;134:230–232.
10. Dawe PS, Flanagan FO, Madekurozwa RL, Sorensen KJ, Anderson EC, *et al.* Natural transmission of foot-and-mouth disease virus from African buffalo (*Syncerus caffer*) to cattle in a wildlife area of Zimbabwe. *Vet Rec* 1994;134:230–232.
11. Gao Y, Sun S-Q, Guo H-C. Biological function of foot-and-mouth disease virus non-structural proteins and non-coding elements. *Viral J* 2016;13:107.
12. Roberts PJ, Belsham GJ. Identification of critical amino acids within the foot-and-mouth disease virus leader protein, a cysteine protease. *Virology* 1995;213:140–146.
13. Vakharia VN, Devaney MA, Moore DM, Dunn JJ, Grubman MJ. Proteolytic processing of foot-and-mouth disease virus polyproteins expressed in a cell-free system from clone-derived transcripts. *J Virol* 1987;61:3199–3207.
14. Moffat K, Knox C, Howell G, Clark SJ, Yang H, *et al.* Inhibition of the secretory pathway by foot-and-mouth disease virus 2BC protein is reproduced by coexpression of 2B with 2C, and the site of inhibition is determined by the subcellular location of 2C. *J Virol* 2007;81:1129–1139.
15. Yost SA, Marcotrigiano J. Viral precursor polyproteins: keys of regulation from replication to maturation. *Curr Opin Virol* 2013;3:137–142.
16. Ferrer-Orta C, Arias A, Agudo R, Pérez-Luque R, Escarmís C, *et al.* The structure of a protein primer-polymerase complex in the initiation of genome replication. *EMBO J* 2006;25:880–888.
17. Birtley JR, Knox SR, Jaulent AM, Brick P, Leatherbarrow RJ, *et al.* Crystal structure of foot-and-mouth disease virus 3C protease. New insights into catalytic mechanism and cleavage specificity. *J Biol Chem* 2005;280:11520–11527.
18. Grubman MJ, Zellner M, Bablanian G, Mason PW, Piccone ME. Identification of the active-site residues of the 3C proteinase of foot-and-mouth disease virus. *Virology* 1995;213:581–589.
19. Forss S, Schaller H. A tandem repeat gene in a picornavirus. *Nucleic Acids Res* 1982;10:6441–6450.
20. King AM, Sangar DV, Harris TJ, Brown F. Heterogeneity of the genome-linked protein of foot-and-mouth disease virus. *J Virol* 1980;34:627–634.
21. González-Magaldi M, Martín-Acebes MA, Kremer L, Sobrino F. Membrane topology and cellular dynamics of foot-and-mouth disease virus 3A protein. *PLoS One* 2014;9:e106685.
22. Ferrer-Orta C, Arias A, Perez-Luque R, Escarmís C, Domingo E, *et al.* Structure of foot-and-mouth disease virus RNA-dependent RNA polymerase and its complex with a template-primer RNA. *J Biol Chem* 2004;279:47212–47221.
23. Herod MR, Gold S, Lasecka-Dykes L, Wright C, Ward JC, *et al.* Genetic economy in picornaviruses: foot-and-mouth disease virus replication exploits alternative precursor cleavage pathways. *PLoS Pathog* 2017;13:e1006666.
24. Ward JC, Lasecka-Dykes L, Neil C, Adeyemi OO, Gold S, *et al.* The RNA pseudoknots in foot-and-mouth disease virus are dispensable for genome replication, but essential for the production of infectious virus. *PLoS Pathog* 2022;18:e1010589.
25. Mason PW, Bezborodova SV, Henry TM. Identification and characterization of a cis-acting replication element (*cre*) adjacent to the internal ribosome entry site of foot-and-mouth disease virus. *J Virol* 2002;76:9686–9694.
26. Kanda T, Ozawa M, Tsukiyama-Kohara K. IRES-mediated translation of foot-and-mouth disease virus (FMDV) in cultured cells derived from FMDV-susceptible and -insusceptible animals. *BMC Vet Res* 2016;12:66.
27. Kloc A, Diaz-San Segundo F, Schafer EA, Rai DK, Kenney M, *et al.* Foot-and-mouth disease virus 5'-terminal S fragment is required for replication and modulation of the innate immune response in host cells. *Virology* 2017;512:132–143.
28. Carrillo C, Tulman ER, Delhon G, Lu Z, Carreno A, *et al.* Comparative genomics of foot-and-mouth disease virus. *J Virol* 2005;79:6487–6504.
29. López de Quinto S, Martínez-Salas E. Conserved structural motifs located in distal loops of aphthovirus internal ribosome entry site domain 3 are required for internal initiation of translation. *J Virol* 1997;71:4171–4175.

30. López de Quinto S, Sáiz M, de la Morena D, Sobrino F, Martínez-Salas E. IRES-driven translation is stimulated separately by the FMDV 3'-NCR and poly(A) sequences. *Nucleic Acids Res* 2002;30:4398–4405.
31. Xiang W, Harris KS, Alexander L, Wimmer E. Interaction between the 5'-terminal cloverleaf and 3AB/3CDpro of poliovirus is essential for RNA replication. *J Virol* 1995;69:3658–3667.
32. Gamarnik AV, Andino R. Interactions of viral protein 3CD and poly(rC) binding protein with the 5' untranslated region of the poliovirus genome. *J Virol* 2000;74:2219–2226.
33. Harris KS, Xiang W, Alexander L, Lane WS, Paul AV, et al. Interaction of poliovirus polypeptide 3CDpro with the 5' and 3' termini of the poliovirus genome. Identification of viral and cellular cofactors needed for efficient binding. *J Biol Chem* 1994;269:27004–27014.
34. Yang Y, Rijnbrand R, Watowich S, Lemon SM. Genetic evidence for an interaction between a picornaviral cis-acting RNA replication element and 3CD protein. *J Biol Chem* 2004;279:12659–12667.
35. Yang F, Zhu Z, Cao W, Liu H, Wei T, et al. Genetic determinants of altered virulence of type O foot-and-mouth disease virus. *J Virol* 2020;94:e01657-19.
36. Kloc A, Rai DK, Rieder E. The roles of Picornavirus untranslated regions in infection and innate immunity. *Front Microbiol* 2018;9:485.
37. Zhu Z, Yang F, Cao W, Liu H, Zhang K, et al. The Pseudoknot region of the 5' untranslated region is a determinant of viral tropism and virulence of foot-and-mouth disease virus. *J Virol* 2019;93:e02039-18.
38. Mohapatra JK, Pawar SS, Tosh C, Subramaniam S, Palsamy R, et al. Genetic characterization of vaccine and field strains of serotype A foot-and-mouth disease virus from India. *Acta Virol* 2011;55:349–352.
39. Escarmís C, Dopazo J, Dávila M, Palma EL, Domingo E. Large deletions in the 5'-untranslated region of foot-and-mouth disease virus of serotype C. *Virus Res* 1995;35:155–167.
40. Paul AV, Rieder E, Kim DW, van Boom JH, Wimmer E. Identification of an RNA hairpin in poliovirus RNA that serves as the primary template in the in vitro uridylylation of VPg. *J Virol* 2000;74:10359–10370.
41. Nayak A, Goodfellow IG, Belsham GJ. Factors required for the uridylylation of the foot-and-mouth disease virus 3B1, 3B2, and 3B3 peptides by the RNA-dependent RNA polymerase (3Dpol) in vitro. *J Virol* 2005;79:7698–7706.
42. Schein CH, Ye M, Paul AV, Oberste MS, Chapman N, et al. Sequence specificity for uridylylation of the viral peptide linked to the genome (VPg) of enteroviruses. *Virology* 2015;484:80–85.
43. Paul AV, Yin J, Mugavero J, Rieder E, Liu Y, et al. A "slide-back" mechanism for the initiation of protein-primed RNA synthesis by the RNA polymerase of poliovirus. *J Biol Chem* 2003;278:43951–43960.
44. Paul AV, Peters J, Mugavero J, Yin J, van Boom JH, et al. Biochemical and genetic studies of the VPg uridylylation reaction catalyzed by the RNA polymerase of poliovirus. *J Virol* 2003;77:891–904.
45. Paul AV, van Boom JH, Filippov D, Wimmer E. Protein-primed RNA synthesis by purified poliovirus RNA polymerase. *Nature* 1998;393:280–284.
46. Belsham GJ, Brangwyn JK. A region of the 5' noncoding region of foot-and-mouth disease virus RNA directs efficient internal initiation of protein synthesis within cells: involvement with the role of L protease in translational control. *J Virol* 1990;64:5389–5395.
47. Bienz K, Egger D, Pfister T, Troxler M. Structural and functional characterization of the poliovirus replication complex. *J Virol* 1992;66:2740–2747.
48. Lundquist RE, Maizel JV. In vivo regulation of the poliovirus RNA polymerase. *Virology* 1978;89:484–493.
49. Barton DJ, Flanagan JB. Synchronous replication of poliovirus RNA: initiation of negative-strand RNA synthesis requires the guanidine-inhibited activity of protein 2C. *J Virol* 1997;71:8482–8489.
50. Richards OC, Martin SC, Jense HG, Ehrenfeld E. Structure of poliovirus replicative intermediate RNA. Electron microscope analysis of RNA cross-linked in vivo with psoralen derivative. *J Mol Biol* 1984;173:325–340.
51. Triantafyllou K, Vakakis E, Kar S, Richer E, Evans GL, et al. Visualisation of direct interaction of MDA5 and the dsRNA replicative intermediate form of positive strand RNA viruses. *J Cell Sci* 2012;125:4761–4769.
52. Goodfellow IG, Polacek C, Andino R, Evans DJ. The poliovirus 2C cis-acting replication element-mediated uridylylation of VPg is not required for synthesis of negative-sense genomes. *J Gen Virol* 2003;84:2359–2363.
53. Morasco BJ, Sharma N, Parilla J, Flanagan JB. Poliovirus cre(2C)-dependent synthesis of VPgpUpU is required for positive- but not negative-strand RNA synthesis. *J Virol* 2003;77:5136–5144.
54. Murray KE, Barton DJ. Poliovirus CRE-dependent VPg uridylylation is required for positive-strand RNA synthesis but not for negative-strand RNA synthesis. *J Virol* 2003;77:4739–4750.
55. Horsington J, Zhang Z. Analysis of foot-and-mouth disease virus replication using strand-specific quantitative RT-PCR. *J Virol Methods* 2007;144:149–155.
56. Plaskon NE, Adelman ZN, Myles KM. Accurate strand-specific quantification of viral RNA. *PLoS One* 2009;4:e7468.
57. Tuiskunen A, Leparc-Goffart I, Boubis L, Monteil V, Klingström J, et al. Self-priming of reverse transcriptase impairs strand-specific detection of dengue virus RNA. *J Gen Virol* 2010;91:1019–1027.
58. Vashist S, Urena L, Goodfellow I. Development of a strand specific real-time RT-qPCR assay for the detection and quantitation of murine norovirus RNA. *J Virol Methods* 2012;184:69–76.
59. Müller M, Slivinski N, Todd E, Khalid H, Li R, et al. Chikungunya virus requires cellular chloride channels for efficient genome replication. *PLoS Negl Trop Dis* 2019;13:e0007703.
60. Tulloch F, Pathania U, Luke GA, Nicholson J, Stonehouse NJ, et al. FMDV replicons encoding green fluorescent protein are replication competent. *J Virol Methods* 2014;209:35–40.
61. Herod MR, Ferrer-Orta C, Loundras E-A, Ward JC, Verdaguer N, et al. Both cis and trans activities of foot-and-mouth disease virus 3D polymerase are essential for viral RNA replication. *J Virol* 2016;90:6864–6883.
62. Loundras E-A, Herod MR, Harris M, Stonehouse NJ. Foot-and-mouth disease virus genome replication is unaffected by inhibition of type III phosphatidylinositol-4-kinases. *J Gen Virol* 2016;97:2221–2230.
63. Herod MR, Loundras E-A, Ward JC, Tulloch F, Rowlands DJ, et al. Employing transposon mutagenesis to investigate foot-and-mouth disease virus replication. *J Gen Virol* 2015;96:3507–3518.
64. Adeyemi OO, Ward JC, Snowden JS, Herod MR, Rowlands DJ, et al. Functional advantages of triplication of the 3B coding region of the FMDV genome. *FASEB J* 2021;35:e21215.
65. Sobrino F, Domingo E. *Foot-and-Mouth Disease Virus: Current Research and Emerging*. Trends: Caister Academic Press; 2017.
66. Li Y, Huang X, Xia B, Zheng C. Development and validation of a duplex quantitative real-time RT-PCR assay for simultaneous detection and quantitation of foot-and-mouth disease viral positive-stranded RNAs and negative-stranded RNAs. *J Virol Methods* 2009;161:161–167.
67. Steil BP, Barton DJ. Cis-active RNA elements (CREs) and picornavirus RNA replication. *Virus Res* 2009;139:240–252.